

Numerical Study of Bubble Flow in Horizontal Perforated Wellbore

Nahid F. Shareef and Mohammed A. Abdulwahid

Thermal Mechanical Engineering, Southern Technical University, Basra, Iraq

Key words: Bubble flow, CFD, two-phase flow, horizontal wells, perforations, pressure drop, homogenous model

Corresponding Author:

Nahid F. Shareef

Thermal Mechanical Engineering, Southern Technical University, Basra, Iraq

Page No.: 224-232

Volume: 16, Issue 5, 2021

ISSN: 1815-932x

Research Journal of Applied Sciences

Copy Right: Medwell Publications

Abstract: In this study, the three-dimensional bubble flow in a horizontal perforated wellbore has been investigated numerically. Unsteady numerical simulations of gas-liquid flow in the horizontal wellbore (of ID= 0.0254 m) have been carried out employing commercial CFD package Fluent 15.1 in conjunction with the VOF model. The turbulence in the continuous phase was described by employing k- ϵ model. Air-water is used as a working fluid in the present work where the air enters from perforations as radial flow and water enters from the mainstream as axial flow. The aim of this study is to investigate the effect of axial and radial flow on the behavior of bubble flow, total pressure drop, void fraction, and friction factor along the horizontal wellbore. The main results revealed that the bubble flow pattern can be seen obviously near the perforations, the friction pressure drop has more effect on total pressure drop compared with mixing pressure drop and acceleration pressure drop, and the void fraction ranges from minimum value to maximum value (0.04-0.526).

INTRODUCTION

Horizontal wells technology became common due to their advantages compared with vertical wells. This includes producing a higher flow rate at lower reservoir pressure drawdown, reduced water coning, and increased well productivity. The perforating horizontal well allows production along the horizontal wellbore. In addition to reducing costs, delaying premature water/gas breakthrough and effectively producing multiple zones with high productivity contrast^[1]. In flow-related industries, determining two-phase flow behavior and measuring it is a major challenge. The void fraction, pressure drop and flow patterns along the pipe are the most important characteristics of two-phase flow^[2]. In the petroleum industry, the flow pattern plays a major role. Most wells thousands of feet below ground level.

Whereby the oil will go through a variety of patterns before it arrives at the surface, each of which will result in a different pressure drop^[3]. In the present study, analyzing bubble flow in the perforated horizontal wellbore to study the significant characteristics of gas-liquid flow. The bubble flow pattern forms at low flow rates of air and intermediate flow rate of water. The bubble flow has great significance in the chemical and process industry where a variety of contacting devices work under the condition of bubble flow to achieve large interfacial areas for heat and mass transfer^[4-6].

Few studies have been carried out to study the bubble flow in horizontal pipes. Yuan *et al.*^[7] a numerical study of bubble flow was implemented along the horizontal reducer pipelines. ANSYS FLUENT with the VOF method is employed in 3D domains to simulate air-water flow. The CFD can be utilized to predict the development

of phase distribution, local and average friction factor and velocity profile. Ekambara *et al.*^[5] a numerical study was conducted for bubble air-water flow in a horizontal pipe to predict the gas volume fraction and mean liquid velocity. Tran^[8] a homogenous model was used to predict the longitudinal distribution of pressure, void fraction and velocity for bubble flow in horizontal pipes. Kocamustafaogullari *et al.*^[4] an experimental study was performed for co-current bubbly flow through a horizontal pipe. The double-sensor resistivity method was used to investigate the local void fraction, size of the bubble, and interfacial area concentration. Yeoh *et al.*^[9] the bubbly air-water flow properties were numerically analyzed in a horizontal pipe. The radial distribution of the air volume fraction, velocity of water and interfacial area concentrations between the two phases was studied. A two-fluid model, together with MUSIC and DQMOM, was used to examine the two fluid's temporal and spatial volume fraction throughout the domain.

Perforated completion is one of the key ways of completion of gas and oil wells and has been commonly implemented worldwide by the oil industry. The significance of perforated completion technology in the discovery and production of petroleum has received growing attention. Perforations are only the passages between the reservoir and the wellbore in oil and gas wells that are completed employing perforating^[10]. The pressure drop in a perforated wellbore has been studied by several researchers whereas the total pressure drop is made up of friction pressure drop, acceleration pressure drop, perforation pressure drop and mixing pressure drop^[11-14]. However, most of the research concentrated on studying friction pressure drop and acceleration pressure drop in horizontal wellbore^[15-17].

Until the present time, few studies have been executed for two-phase flow in the perforated horizontal wellbore to calculate the pressure drop using air and water as working fluids^[18-20]. Wen *et al.*^[18] numerical and experimental study were performed in horizontal wells. The main results revealed, the pressure drop during the perforation process increased with the perforation main pipe flow ratio at the same total flow rate and increased with increasing axial velocity while radial velocity remained constant for a single-phase and two-phase. Hua *et al.*^[19] improved the pressure drop model for changeable mass flow in the horizontal wellbore. The results showed the friction pressure drop had more influence on total pressure drop than the acceleration pressure drop and mixture pressure drop. The fluid viscosity has a greater influence on total pressure drop and friction pressure drop where both types of pressure drop increasing with increased liquid viscosity in comparison with acceleration pressure drop and mixing pressure drop in the horizontal wellbore. Liu *et al.*^[20] the distribution of pressure in horizontal gas well with various

inflow media, perforation opening methods and various liquid holdup was investigated numerically. The main results revealed that the pressure close to the cluster of perforation increased when the inflow of perforation and the cluster number increased. No significant change in overall pressure when the existing perforations uniform or non-uniform and the pressure increased significantly when the liquid holdup <0.5 and fluctuates greatly close to the first perforation when liquid holdup >0.5. Most previous research has concentrated on pressure drop in the horizontal perforated wellbore, up to my knowledge, no numerical study transacted with bubble flow pattern in the perforated horizontal wellbore.

The main objectives of the present study are using CFD to simulate the bubble flow in the perforated horizontal wellbore to calculate the total pressure drop which includes (friction pressure drop, mixing pressure drop and acceleration pressure drop), the productivity rate, distribution of volume fraction and friction factor at various cross-sections along the horizontal wellbore.

MATERIALS AND METHODS

Numerical procedures

Description of model and assumptions: The physical model is employed in numerical simulation is a horizontal section of the wellbore with 0.0254 m inner diameter and of 2 m length. The test section has fourteen perforations distributed equally along the wellbore with a 0.25 m distance, these perforations with an inner diameter of 0.004 m with perforations phase 180°. The superficial velocity of air (radial velocity) is 0.12 m sec⁻¹ but the superficial velocity of water (axial velocity) is 0.25 m sec⁻¹. The model description is illustrated in Fig. 1.

The following assumptions have been used in the present model solution:

- The fluid is Newtonian
- The flow is turbulent, unsteady and incompressible
- Three-dimensional geometry in numerical analysis is the same as used in experimental work
- The working fluids are air (radial flow) and water (axial flow)
- The body force is neglected
- The properties of fluid flow are constant
- The system is isothermal

CFD ANSYS fluent: ANSYS FLUENT 15.1 with the finite volume method is employed. The Volume of Fluid (VOF) homogenous model is used to solve the geometry of 3D. The unstructured mesh is used, tetrahedral mesh with 340,468 nodes and 1,081,963 elements as shown in Fig. 2. Besides, for turbulence closure, the Realizable

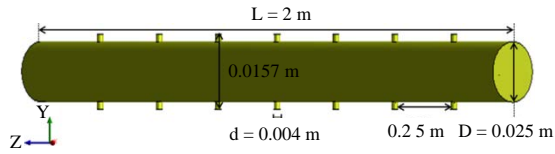


Fig. 1: Schematic drawing of test section

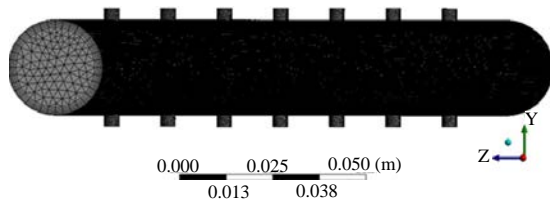


Fig. 2: Meshing model of a horizontal perforated wellbore

Table 1: Boundary condition

| Location | Boundary condition | Comments |
|-------------|---|--|
| At inlet | $u = U_{sw} = in$ and $\alpha_q = 0$ $v = U_{sa} = in_1, in_2, \dots$ and $in_{1,4}$ and $\alpha_q = 1$ | Velocity inlet and Volume fraction for secondary phase |
| At outlet | $dU/dx = dV/dy = dW/dz = 0, p = 0$ | Pressure outlet |
| At the wall | $U = V = W = 0$ | No-slip condition |

model of k-ε with five inflation layers of cells is located near the pipe wall to ensure that the correct simulation will transpire near the wall. The calculations were performed by a combination of the Semi-Implicit Pressure-Linked Equation solver (SIMPLE) algorithm for pressure-velocity coupling to enforce mass conservation and to obtain the pressure field.

Initial and boundary conditions

Initial condition: All starting conditions of air and water flow are set to zero velocity ($t = t_0, v = v_0$) at $t = 0$ sec. Also, specified the volume fraction of air ($\alpha_a = 0$). This means that initially the domain was filled with water. Air was then introduced from the perforations inlet at a constant velocity.

Boundary conditions

The two-phase flow model: For a description of gas-liquid slug two-phase flow behavior, the Volume of Fluid (VOF) method in commercial Fluent 15.1 CFD software is used (Table 1). This model depends on Navier-Stokes equations to analyzing mixture flow, unsteady state and turbulent flow for 3D geometry. The steady or transient formulation of VOF depends on the absence of the interpenetration of two or more fluids (or phases). For each control volume, the total of the volume fractions of all phases is equal to one in the entire numerical calculation. At each location, the volume fraction of liquid and gas is known. So, in any given cell,

depending upon the values of volume fraction, the variables and characteristics are purely representative of one of the phases or representative of the mixture of the phases. Likewise different words, if the q_{th} fluid's volume fraction in the cell is referred to as α_q , then there are three different conditions^[21]:

- $\alpha_q = 0$: the cell is empty (of the fluid)
- $\alpha_q = 1$: the cell is full (of the q_{th} fluid)
- $0 < \alpha_q < 1$: the cell includes the interface between the fluid and one or more of the other fluids available

In the VOF model, the density of the mixture ρ_m and dynamic viscosity of the mixture μ_m are estimated as follows:

$$\rho_m = \rho_g \alpha_q + \rho_l (1 - \alpha_q) \quad (1)$$

$$\mu_m = \mu_g \alpha_q + \mu_l (1 - \alpha_q) \quad (2)$$

where subscripts l and g indicate the liquid phase and gas phase, respectively.

Governing equations: Numerical simulation of any flow problem is focused on solving the fundamental flow equations that explain turbulence, mass and momentum for two-phase flow, those are called Navier-Stokes equations. Also, the volume of the fraction conservation equation for each phase through the domain. For each phase, the principle equations are solved and can be written as follow:

Mass conservation: A continuity equation solution for the volume fraction of one (or more) of the phases. For the q_{th} phase, the following form of this equation is given by Patel^[22]:

$$\frac{\partial}{\partial t} (\alpha) + \nabla \cdot (\alpha \bar{V}_m) = 0 \quad (3)$$

Continuity equation of the mixture at unsteady state as given by Razavi:

$$\frac{\partial}{\partial t} (\rho) + \nabla \cdot (\rho \bar{V}_m) = 0 \quad (4)$$

The mass equation in three dimensions:

$$\frac{\partial \rho_m}{\partial t} + \frac{\partial (\rho_m U_m)}{\partial x} + \frac{\partial (\rho_m V_m)}{\partial y} + \frac{\partial (\rho_m W_m)}{\partial z} = 0 \quad (5)$$

Conservation of momentum: The momentum equation is based on volume fractions of all phases through the properties ρ_m and μ_m as shown below^[23, 24]:

$$\frac{d}{dt}(\rho_m \bar{V}_m) + \nabla \cdot (\rho_m \bar{V}_m \bar{V}_m) = -\nabla P + \rho_m \bar{g} + \nabla \cdot [\mu_m (\nabla \bar{V}_m + \nabla \bar{V}_m^T)] + \bar{F}$$
(6)

Where:

$[\mu_m (\nabla \bar{V}_m + \nabla \bar{V}_m^T)]$ = The viscous stress tensor
 \bar{F} = The identity interaction between phases across the interface

Total pressure drop: The total pressure drop horizontal perforated wellbore consists of four terms: acceleration pressure drop, friction pressure drop, perforation roughness pressure drop and mixing pressure drop as illustrated in the following relationship:

$$\Delta p = \Delta p_{wall} + \Delta p_{acc.} + \Delta p_{perf.} + \Delta p_{mix}$$
(7)

Where:

Δp = Total pressure drop (pa)
 Δp_{wall} = Wall friction pressure drop (pa)
 Δp_{acc} = Acceleration pressure drop (pa)
 Δp_{perf} = Perforation roughness pressure drop (pa)
 Δp_{mix} = Mixing pressure drop (pa)

To calculate the four types of pressure drops of the two-phase flow, it was considered the same laws of single-phase by replacing the variables with equivalent variables of two-phase as shown in the following equations given by Su and Gudmundsson^[25], Zhang *et al.*^[26] and Asheim *et al.*^[27]:

$$\Delta p_{wall} = \frac{f_p \rho_m U_m^2 \Delta x}{2D}$$
(8)

$$\Delta p_{acc.} = 2\rho_m U_m \frac{q_p}{A} - \rho_m \left(\frac{q_p}{A}\right)^2$$
(9)

$$\Delta p_p = \frac{f_p \rho_m U_m^2 \Delta x}{2D}$$

$$\Delta p_{mix} = \begin{cases} \Delta p_p - 0.031 Re_{(2ph)} \xi_p (\xi_p \leq 0.1) \\ 760 \xi_p (\xi_p > 0.1) \end{cases}$$
(10)

$$f_p = 4D \frac{q_L}{q} + 2 \frac{D}{n} \left(\frac{q_L}{q}\right)^2$$
(11)

Where:

ξ_p = The ratio of inflow rate through one perforation to main flow rate
 q_L = Inflow rate per unit length (m³/s/m)
 q_p = Inflow rate through each perforation (m³ sec⁻¹)
 q = Main flow rate (m³ sec⁻¹)
 f_p = Equivalent friction factor due to influx
 n = Perforation density (m⁻¹)

Where:

$$\xi_p = \frac{q_p}{q}$$
(12)

$$q_L = n v_p \pi d^2 / 4$$
(13)

To calculate the total effective friction factor is equal to the sum of perforation friction factor and wall friction factor as given by Asheim *et al.*^[27]:

$$f = f_w + f_p$$
(14)

Depending on Eq. 14, the total friction pressure drop can be calculated by summation wall friction pressure drop and perforation pressure drop.

RESULTS AND DISCUSSION

Simulation of bubble flow pattern in perforated horizontal wellbore: Figure 3 explains the behavior of the bubble flow pattern for all perforations along the pipe when the air superficial velocity equal to 0.12 m sec⁻¹ and water superficial velocity equal to 0.25 m sec⁻¹. In perforated pipes, the bubble flow pattern observes near the perforations, this agree with. That shows clear close to the lower perforations but the radial inflow from upper perforations concentrated in the upper part of the wellbore because of the difference in density and viscosity of the mixture.

Bubble flow behavior: The behavior of bubble flow pattern in a perforated horizontal wellbore for the last two perforations from the horizontal wellbore is illustrated in Fig. 4. Water is considered the primary phase, that enters from the mainstream (axial flow) while air is considered the secondary phase that enters from perforations (radial flow). For the primary phase in the inlet boundary condition, the volume fraction of inlet air is 0; the volume fraction of inlet water is 1. For the secondary phase, the volume fraction of inlet air is 1 and the volume fraction of inlet water is 0. Figure 4 explains the behavior of bubble flow, at the initial time the wellbore filled with water by assuming the volume fraction of air is 0, that's mean the volume fraction of water is 1. Air entering from the perforations along the wellbore at the same time with the same flow rate. At time 0.38 sec, the gas bubbles are rising during the horizontal wellbore. From time 1.17-3.03 sec, the gas bubbles continue rising due to buoyancy force and accumulated at the top of the wellbore, then combined with the other bubbles of gas from upper perforations. From time 4.22-8.3 sec, the same behavior as with the previous step except the shape of bubbles changes due to increase gas superficial velocity during the wellbore.

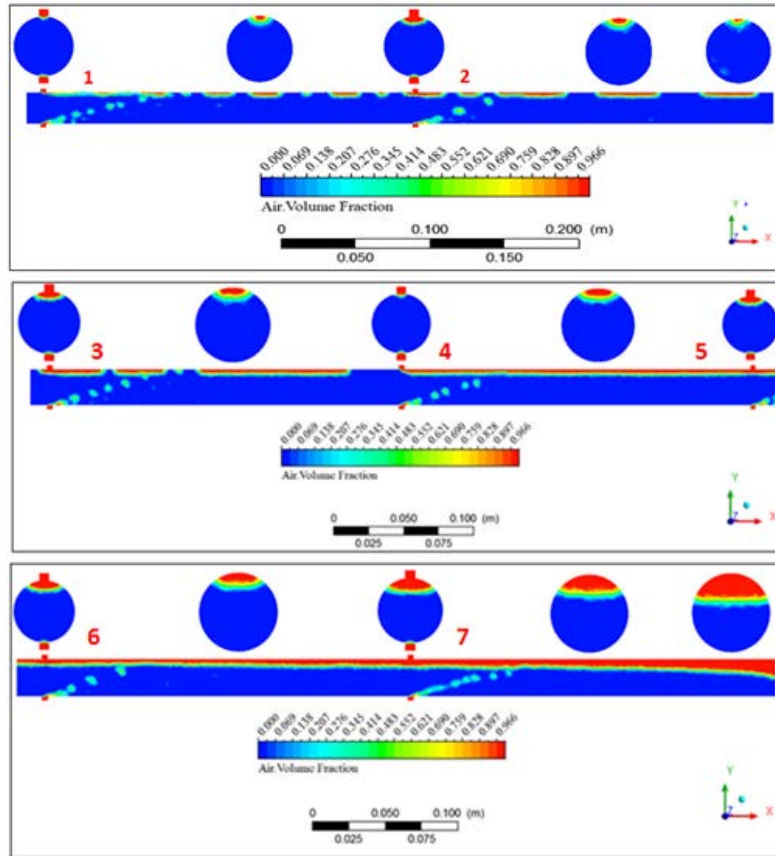


Fig. 3: Cross-section of the fluid domain for the extraction of volume fraction at time 8.34 sec

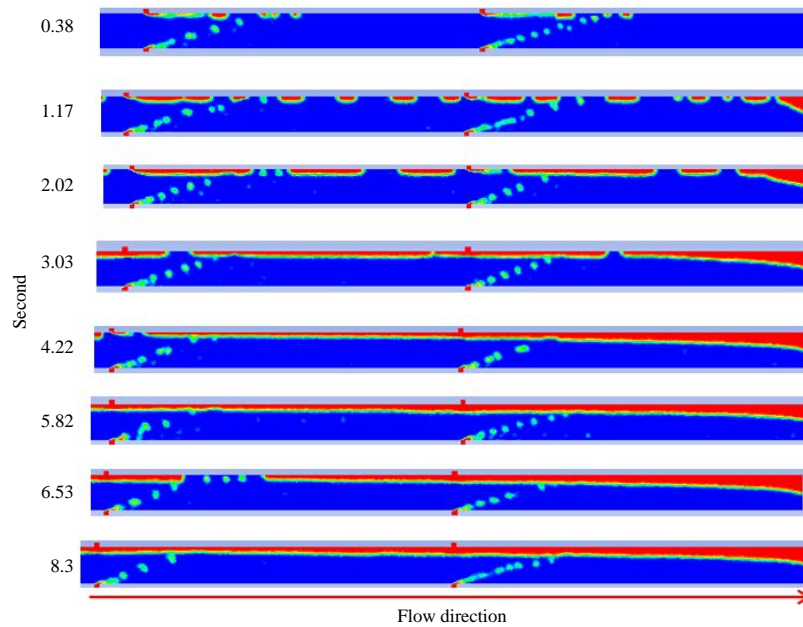


Fig. 4: Behavior of bubble flow pattern which formed over time 8.3 sec in the horizontal perforated wellbore at the x-y plane

Pressure drop in Bubble flow: The total pressure drop in the horizontal wellbore consists of friction pressure drop (which contains the wall friction and perforation roughness pressure drops), acceleration pressure drop and mixing pressure drop. Figure 5 illustrates the distribution of pressure drop along the horizontal wellbore. Generally, the values of pressure drop relatively small because of the small flow rates of air and water, where the total pressure drop consists of 69.4% friction pressure drop, 21.4% mixing pressure drop and 9.12% acceleration pressure drop. The results showed the distribution of pressure fluctuated along the wellbore because of continuous inflow from the reservoir to the wellbore, at the position of perforations pressure drop increase when radial inflow mix with the axial flow in the wellbore. So, the void fraction increases in this area because of the increasing air flow rate. As a result, the viscosity and the density of the mixture decrease, so the pressure decrease in the position of perforation and close to the heel of the well. Figure 6 shows the distribution of static pressure along the horizontal wellbore and corresponding static pressure contour illustrates in Fig. 7. It is observed from the results of the pressure decrease gradually from the toe of the well to the heel of the well. The higher static pressure is shown in the bottom part of the wellbore as illustrates in Fig. 7 because of higher density and viscosity in this area.

Productivity in horizontal wellbore: Figure 8 demonstrates the variation of flow rate along the

horizontal wellbore. It is observed from the results, the flow rates increase along the horizontal wellbore because of the continuous inflow from the reservoir through the perforations into the wellbore. It is observed the decrease in flow rate at the position of perforations because of the air flow rate more than the water flow rate in this area. After the position of perforations, the flow rate increases gradually when the radial flow rate from perforation (air flow) mixes with the axial flow in the wellbore (water flow) until reaching the maximum value close to the heel of well.

Distribution of volume fraction: Figure 9 illustrates the distribution of the void fraction for the bubble flow pattern at various positions along the wellbore, Fig. 9a pointed to distribution void fraction at the midpoint between 1-5 perforations while Fig. 9b pointed to distribution void fraction at the midpoint between 5-7 perforation. The results showed the void fraction increases in the top of the wellbore where the gas bubbles rising due to the effect of gravity and buoyancy force on the horizontal wells. Whereas the void fraction in the bottom of the wellbore decreases until reaches zero because of more amount of water accumulated at the bottom due to the difference in density, on contrary, the liquid holdup will increase.

Whilst the distribution of the void fraction is significantly different near the perforations because of increasing the gas bubbles that rising from bottom perforations as explains in Fig. 10.

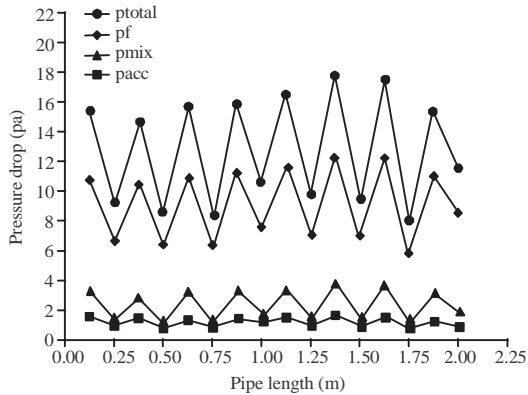


Fig. 5: Distribution of pressure drop along the horizontal wellbore in bubble flow

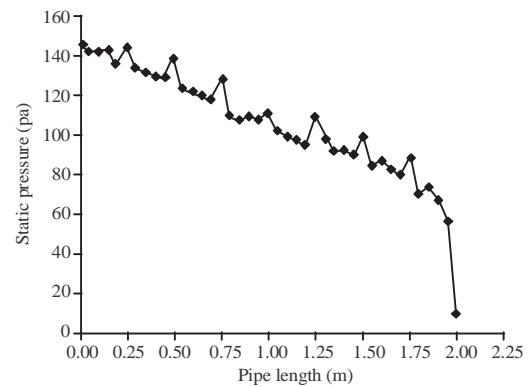


Fig. 6: Static pressure along horizontal wellbore in bubble flow

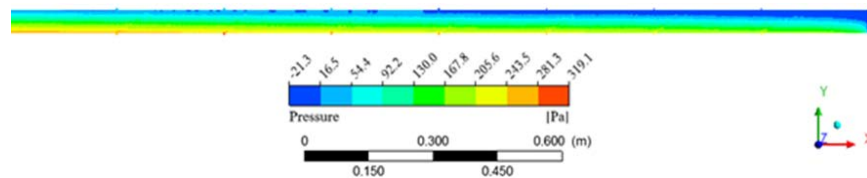


Fig. 7: Static pressure contour along horizontal wellbore in bubble flow

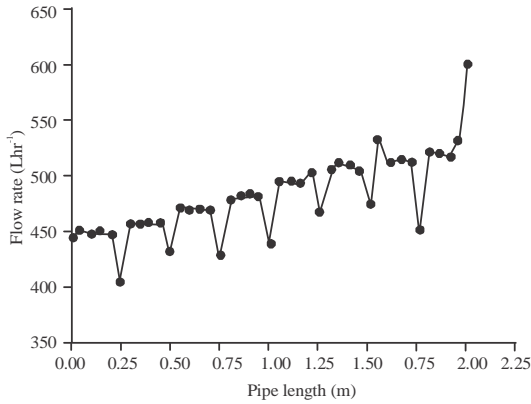


Fig. 8: Productivity along the horizontal wellbore in bubble flow

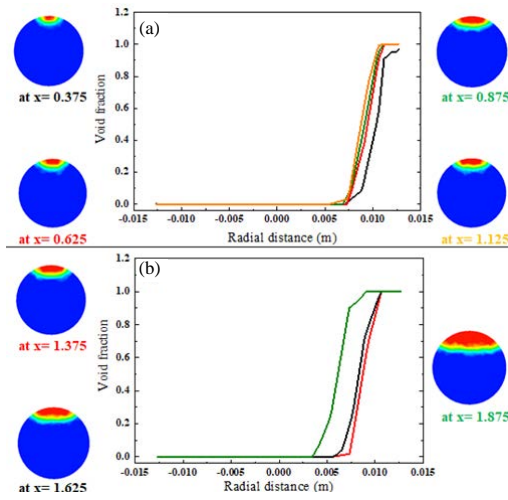


Fig. 9: Distribution of void fraction in bubble flow

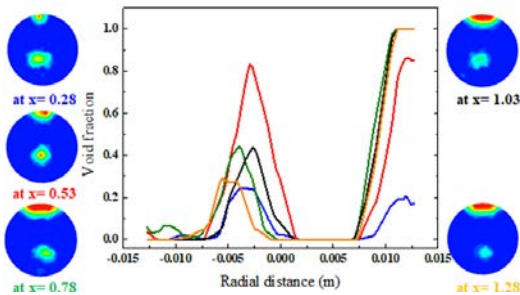


Fig. 10: Distribution of void fraction of bubble flow near perforation

Figure 11 presents the distribution of volume fraction along the horizontal wellbore. Figure 11a pointed to distribution void fraction, Fig. 11b pointed to distribution liquid holdup along the wellbore. The results showed the void fraction increases at the position of the perforations due to the continuous air inflow from the

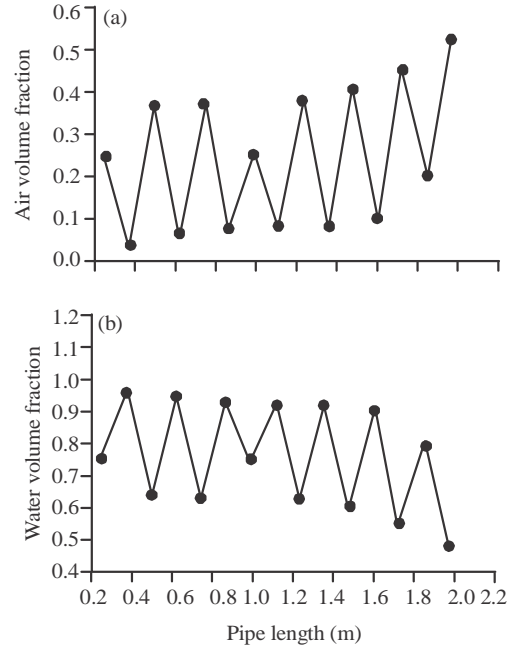


Fig. 11(a, b): Distribution of volume fraction of bubble flow along the wellbore

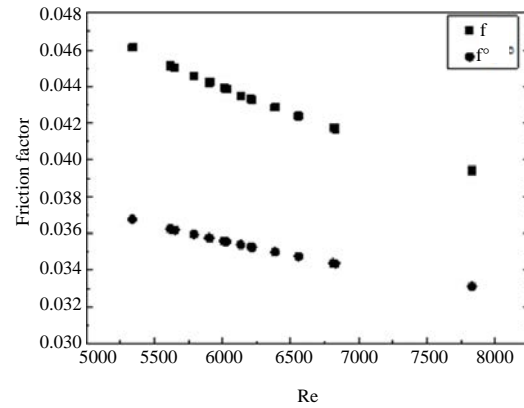


Fig. 12: Friction factor of two-phase flow versus Reynolds number in bubble flow

perforations. The value of the void fraction at the range of 4-52.67% where the maximum value of void fraction at the heel of the wellbore because more flow rate of air from all perforations accumulated in this area. While the liquid holdup is the reverse value of the void fraction as illustrated in Fig. 11 b. The liquid holdup decreases in the position of perforations due to increasing air volume fraction leads to a decrease in the liquid film thickness as a result the liquid holdup decrease.

Friction factor of two-phase flow in bubble flow: Figure 12 illustrates the friction factor versus Reynolds number. Where the friction factor includes the wall

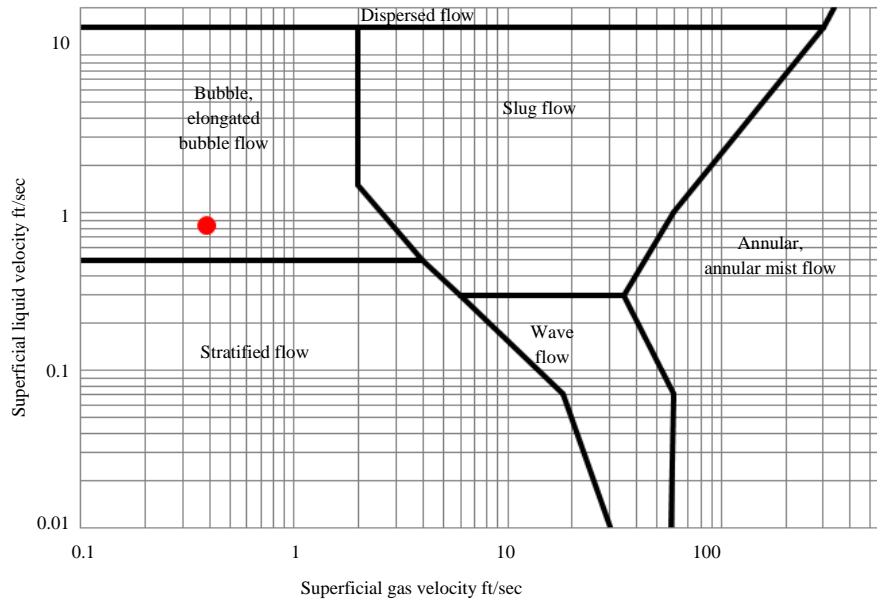


Fig. 13: Flow pattern map of two-phase in horizontal flow

friction factor (f_o) and total friction factor (f) which product from the sum of the wall friction factor and perforation friction factor. It observes that the friction factor increases with a decrease in the Reynolds number. Where the friction factor in range (0.0327-0.035) the total friction factor in the range (0.0394-0.0461) corresponding to the minimum and maximum values of Reynolds number, respectively 5338.8 and 7830.86. The proportion of increment of friction factor along the perforated horizontal wellbore is relatively small, that because the change in mixture velocity for bubble flow is very small, so the Reynolds number values are convergent too.

Flow pattern map of two-phase flow: Figure 13 presents the flow pattern of the two-phase flow. Figure 13 indicates the bubble flow which is used in the present study at a gas superficial velocity of 0.12 m sec^{-1} and liquid superficial velocity is 0.25 m sec^{-1} . The results reveal a good agreement between the data used in the present study and the flow pattern map of the two-phase in horizontal pipe introduced by Mandhane *et al.*^[28].

CONCLUSION

The main conclusions were drawn from a numerical simulation of the bubble flow pattern in a horizontal perforated wellbore: The Realizable (k-e) model with unsteady-state is used to numerically simulate bubble turbulent two-phase air-water flow in the horizontal perforated wellbore using ANSYS FLUENT IN combination with the VOF system. Although, the current

formulation is very difficult due to the need for fine grids and more computational time, it appears that the CFD method can be used to efficiently model bubble flow patterns numerically. The void fraction has a fewer effect on the pressure drop where the value of the void fraction is relatively small.

The value of the total pressure drop is quite small in the bubble pattern where the friction pressure drop represents the highest percentage in the total pressure drop. Then the mixing pressure drop and the lowest percentage in the total pressure drop is the acceleration pressure drop. The static pressure decreases with the increasing of mixture velocity along the horizontal wellbore.

Wall friction factor increases when the mixture velocity decrease whereas the equivalent friction factor due to influx increases when the perforations velocity increase.

REFERENCES

01. Guo, X. and T. Shi, 2006. Productivity of selectively open horizontal wells. *SPE Prod. Oper.*, 21: 75-80.
02. Jagan, V. and A. Satheesh, 2016. Experimental studies on two phase flow patterns of air-water mixture in a pipe with different orientations. *Flow Meas. Instrum.*, 52: 170-179.
03. Wang, Y., 2018. A study of two-phase flow regime and pressure drop in vertical pipe. Master Thesis, University of North Dakota, Grand Forks, North Dakota.

04. Kocamustafaogullari, G., W.D. Huang and J. Razi, 1994. Measurement and modeling of average void fraction, bubble size and interfacial area. *Nucl. Eng. Des.*, 148: 437-453.
05. Ekambara, K., R.S. Sanders, K. Nandakumar and J.H. Masliyah, 2008. CFD simulation of bubbly two-phase flow in horizontal pipes. *Chem. Eng. J.*, 144: 277-288.
06. Andreussi, P., A. Paglianti and F.S. Silva, 1999. Dispersed bubble flow in horizontal pipes. *Chem. Eng. Sci.*, 54: 1101-1107.
07. Yuan, W., S. Liu, S. Li, T. Tao and K. Xin, 2011. Numerical simulation of bubble motion in horizontal reducer pipelines. *Eng. Appl. Comput. Fluid Mech.*, 5: 517-529.
08. Tran, P.D., 2008. Distributions of pressure, velocity and void fraction for one-dimensional gas-liquid bubbly flow in horizontal pipes. *J. Fluids Eng.*, 130: 0913021-0913029.
09. Yeoh, G.H., S.C. Cheung and J.Y. Tu, 2012. On the prediction of the phase distribution of bubbly flow in a horizontal pipe. *Chem. Eng. Res. Des.*, 90: 40-51.
10. Renpu, W., 2011. Perforating. In: *Advanced Well Completion Engineering*, Renpu, W. (Ed.), Elsevier, Amsterdam, Netherlands, pp: 295-363.
11. Su, Z. and J.S. Gudmundsson, 1994. Pressure drop in perforated pipes: experiments and analysis. *Proceedings of the SPE Asia Pacific Oil and Gas Conference*, November 7-10, 1994, Society of Petroleum Engineers, Melbourne, Australia, pp: 563-574.
12. Su, Z. and J.S. Gudmundsson, 1998. Perforation inflow reduces frictional pressure loss in horizontal wellbores. *J. Pet. Sci. Eng.*, 19: 223-232.
13. Abdulwahid, M.A., S.F. Dakhil and N.K. Injeti, 2013. Numerical investigation of the turbulent flow parameters distribution in a partly perforated horizontal wellbore. *Eur. Sci. J.*, 9: 372-387.
14. Abdulwahid, M., N. Kumar and S. Dakhil, 2014. A comparison of the density perforations for the horizontal wellbore. *WSEAS Trans. Fluid Mech.*, 9: 110-115.
15. Sarica, C., M. Haciislamoglu, R. Raghavan and J.P. Brill, 1994. Influence of wellbore hydraulics on pressure behavior and productivity of horizontal gas wells. *Proceedings of the SPE Annual Technical Conference and Exhibition*, September 25-28, 1994, Society of Petroleum Engineers, New Orleans, Louisiana, pp: 237-247.
16. Landman, M.J., 1994. Analytic modelling of selectively perforated horizontal wells. *J. Pet. Sci. Eng.*, 10: 179-188.
17. Novy, R.A., 1995. Pressure drops in horizontal wells: When can they be ignored?. *SPE Reservoir Eng.*, 10: 29-35.
18. Wen, J., M. Yang, W. Qi, J. Wang, Q. Yuan and W. Luo, 2018. Experimental analysis and numerical simulation of variable mass flow in horizontal wellbore. *Int. J. Heat Technol.*, 36: 309-318.
19. Hua, L., L. Yan, P. Xiaodong, L. Xindong and W. Laichao, 2016. Pressure drop calculation models of wellbore fluid in perforated completion horizontal wells. *IJHT. Int. J. Heat Technol.*, 34: 65-72.
20. Liu, J., Z. Jiang, X. Feng, R. Liao, D. Feng and X. Zhang, 2020. An experimental study on pressure distribution in the horizontal gas wells. *Fluid Dyn. Mater. Process.*, 16: 1243-1258.
21. Azadi, M., S.M. Aminossadati and Z. Chen, 2017. Development of an integrated reservoir-wellbore model to examine the hydrodynamic behaviour of perforated pipes. *J. Pet. Sci. Eng.*, 156: 269-281.
22. Patel, G.N., 2010. CFD simulation of two-phase and three-phase flows in internal-loop airlift reactors. *Master's Thesis*, Department of Mathematics and Physics, Lapeenranta University of Technology, Lapeenranta, Finland.
23. Peng, H. and X. Ling, 2008. Numerical simulation on pressure drops for air-water two-phase flow in micro-channels. *Proceedings of the International Conference on Micro/Nanoscale Heat Transfer*, June 6-9, 2008, ASME, Tainan, Taiwan, pp: 997-1004.
24. Ranade, V.V., 2002. *Computational Flow Modeling for Chemical Reactor Engineering*. Academic Press, San Diego, CA, USA., pp: 452.
25. Su, Z. and J.S. Gudmundsson, 1993. Friction factor of perforation roughness in pipes. *Proceedings of the SPE Annual Technical Conference and Exhibition*, October 3-6, 1993, Society of Petroleum Engineers, Houston, Texas, pp: 151-163.
26. Zhang, Q., Z. Wang, X. Wang and J. Yang, 2014. A new comprehensive model for predicting the pressure drop of flow in the horizontal wellbore. *J. Energy Resour. Technol.*, Vol. 136, No. 4. 10.1115/1.4027572
27. Asheim, H., J. Kolnes and P. Oudeman, 1992. A flow resistance correlation for completed wellbore. *J. Pet. Sci. Eng.*, 8: 97-104.
28. Mandhane, J.M., G.A. Gregory and K. Aziz, 1974. A flow pattern map for gas-liquid flow in horizontal pipes. *Int. J. Multiphase Flow*, 1: 537-553.